



# AVERAGE MODEL RESEARCH FOR CAPS MMC

## Technical Report

Submitted to:  
The Office of Naval Research

Contract Number: N00014-16-1-2956

Submitted by:  
L. Wang, Y. Shi, D. Soto, J. Langston, K. Schoder, J. Hauer, and M. Steurer

Oct. 2019

-



## MISSION STATEMENT

The Electric Ship Research and Development Consortium brings together in a single entity the combined programs and resources of leading electric power research institutions to advance near-to mid-term electric ship concepts. The consortium is supported through a grant from the United States Office of Naval Research.



2000 Levy Avenue, Suite 140 | Tallahassee, FL 32310 | [www.esrdc.com](http://www.esrdc.com)

## TABLE OF CONTENTS

<b>1</b>	<b>Introduction</b>	<b>3</b>
<b>2</b>	<b>MMC Switching Model Simplified by Average Model</b>	<b>3</b>
2.1	Switching model introduction . . . . .	4
2.2	Average model introduction . . . . .	4
2.3	Simulation results comparison between SWM and AVM . . . . .	4
<b>3</b>	<b>Average Modeling by Impedance Shaping</b>	<b>7</b>
3.1	MMC back to back tests . . . . .	7
3.2	Impedance shaping for current control mode MMC . . . . .	8
3.3	Impedance shaping for voltage control mode MMC . . . . .	11
<b>4</b>	<b>Average Model Verification and Validation</b>	<b>15</b>
4.1	MMC current transient . . . . .	15
4.2	MMC voltage transient . . . . .	17
4.3	MMC short circuit operation . . . . .	19
<b>5</b>	<b>Conclusion</b>	<b>22</b>
<b>6</b>	<b>Future Work</b>	<b>22</b>
	<b>References</b>	<b>24</b>
<b>A</b>	<b>Attached Matlab Model list</b>	<b>25</b>

## LIST OF FIGURES

1	MMC SWM and AVM with the same references, identical control loop and parameters. . . . .	4
2	MMC switching model. . . . .	5
3	MMC average model. . . . .	5
4	MMC SWM and AVM simulation results comparison. . . . .	7
5	MMC back to back testbed configuration. . . . .	8
6	AVM at current control mode. . . . .	9
7	Current control mode MMC impedance from test [1]. . . . .	10
8	Current control mode MMC impedance measurement from AVM. . . . .	10
9	Current control mode MMC impedance shaping with different zeros. . . . .	12
10	AVM at voltage control mode. . . . .	13
11	Voltage control mode MMC impedance from test [1]. . . . .	14
12	Voltage control mode MMC impedance measurement from AVM. . . . .	14
13	Current control mode MMC current 0-200 A step response comparison (at 5 kV). . . . .	15

14	Current transient comparison between AVM and CHIL. . . . .	16
15	Percentage of error in rise time between CHIL and AVM. . . . .	16
16	Voltage control mode MMC voltage 0-5 kV step response comparison (at 200 A). .	17
17	Voltage transient comparison between AVM and CHIL. . . . .	19
18	MMC short circuit test configuration. . . . .	19
19	Single MMC voltage control mode short circuit comparison (at 5 kV open circuit).	20
20	Short circuit comparison between AVM and CHIL. . . . .	21
21	AVM short circuit operation errors. . . . .	21
22	Statistic of measured rise time in CHIL. . . . .	23
23	Statistic of measured rise time from experiments with two B2B 1.25MW MMCs. .	23
24	Example of a power converter modelability study . . . . .	24

## LIST OF TABLES

1	MMC parameters . . . . .	6
2	Voltage transient cases . . . . .	18

# 1 INTRODUCTION

This report details the development of a simplified average model (AVM) for an MMC at CAPS. The AVM can emulate the steady state and transient behaviors seen in experimental results. The purpose of the model is to achieve less complexity and faster time domain simulation studies of the MMCs at CAPS, while still maintaining sufficient converter dynamic accuracy. The method utilized applies equivalent circuit models of the power stage and the duty-cycle generation circuitry to describe the low frequency behavior of switching model (SWM) systems.

Unlike the conventional white box method to build up the AVM with all the control information available, an impedance shaping method was used. The idea of the impedance shaping method is to build the AVM from a black box, with only the measured impedance results. The method in this report is much simpler than the conventional one, without exposing the internal control information. The control algorithm and control methods are modeled based on the impedance shaping results. The saturation limitations in the controller are designed based on the system transient.

In Section 2, a MMC SWM model is compared with a AVM model, with the same reference, identical control loops and system parameters. The step response and the short circuit transient are well matched between two models and validated that AVM is able to represent the SWM of the MMC. In Section 3, MMC current control loop and voltage control loop is presented. AVM is designed by impedance shaping based on the MMC measured impedance from [1]. In Section 4, the time domain transient results from the AVM are compared with the CHIL test results, including the current step, voltage step, and the short circuit operation. The verification and validation is implemented at different operation conditions.

## 2 MMC SWITCHING MODEL SIMPLIFIED BY AVERAGE MODEL

As shown in Fig. 1, a SWM and a AVM for MMC were built in Matlab/Simulink. For both models, the same ac and dc references, control loops and parameters are utilized. The input for the models are the dc reference voltage  $d$  and the ac reference voltage  $m$ . The MMC dc-link voltage equation is given by (1) and ac output voltage by (2), where  $N$  is the number of cells,  $\omega_0$  is the fundamental frequency and  $\theta_0$  is the phase angle. The outputs of the models are the dc voltage  $v_{dc}$ , dc current  $i_{dc}$ , and the ac current  $i_{ac}$ .

$$v_{dc} = 2dNV_{cell} \quad (1)$$

$$v_{ac} = 2mNV_{cell}, m = \cos(\omega_0 t + \theta_0) \quad (2)$$

With identical  $d$ ,  $m$  inputs and controls, if the output waveforms of SWM and AVM match, then the SWM can be simplified by AVM. With a AVM, the switching operations at the power stage can be neglected and the circuit can be simulated much faster.

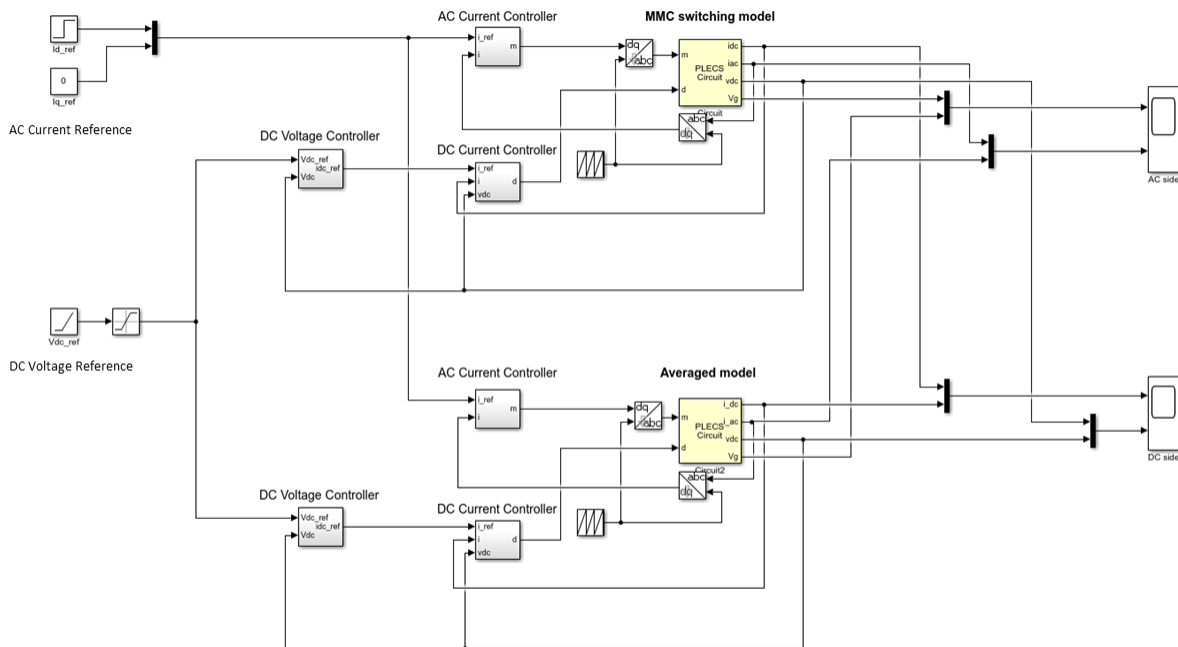


Fig. 1: MMC SWM and AVM with the same references, identical control loop and parameters.

## 2.1 Switching model introduction

The SWM was built based on the MMC available at CAPS [2], which have a similar structure as the model shown in Fig. 2. They are built with six arms, each arm consisting of six full-bridge cells in series. A coupled inductor is connected in each phase to reduce the dc ripple. Carried based phase shifted pulse width modulation is applied. The ac and dc voltage waveforms contain the switching frequency information.

## 2.2 Average model introduction

The ac loop and the dc loop are modeled separately in the AVM, as shown in Fig. 3. The dc loop is fully decoupled from the ac loop in this model. The ac loop contains controllable ac voltage source, ac inductors, and the ac grid. The dc loop contains controllable dc voltage source, dc inductors, and a resistive load. Switching related components are not utilized.

## 2.3 Simulation results comparison between SWM and AVM

For this simulation, both models are running with ac and dc closed-loop current control and the voltage loop is disabled. The ac side is connected to the grid and the dc side is connected to a resistive load. The MMC parameters are listed in Table 1.

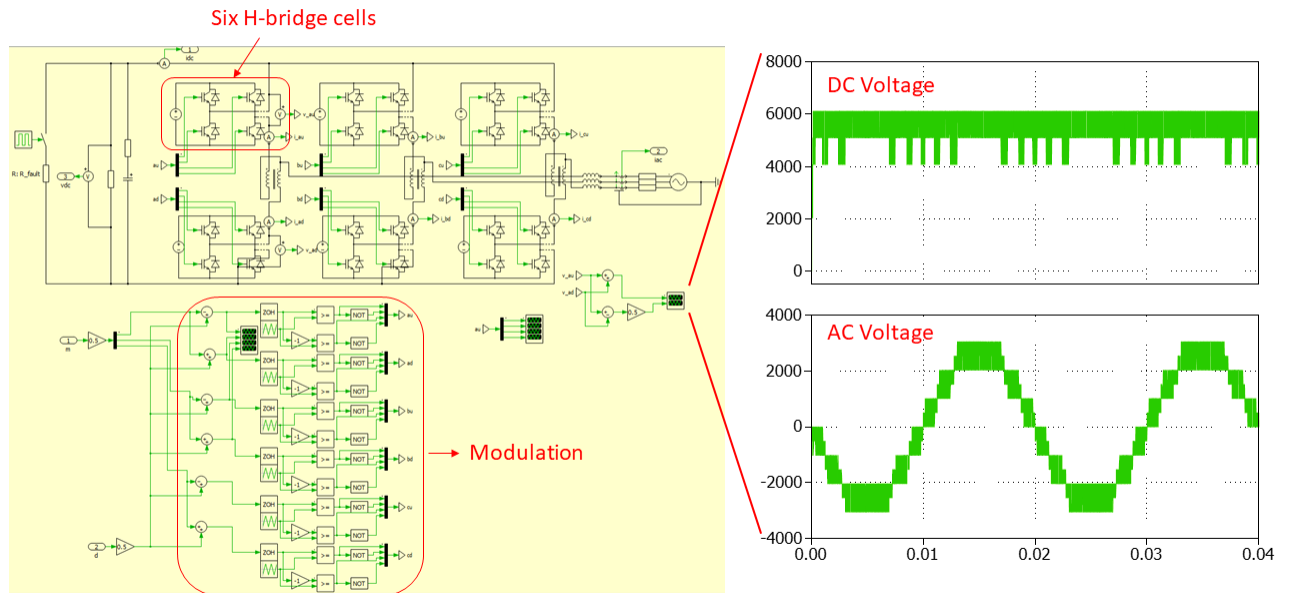


Fig. 2: MMC switching model.

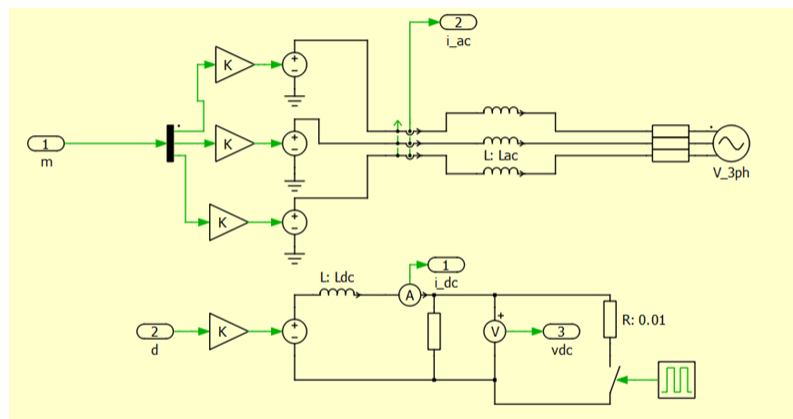


Fig. 3: MMC average model.

Table 1: MMC parameters

<b>Parameter</b>	<b>Value</b>
Power rating	1.25 MW
DC voltage base	6 kV
DC current base	208 A
AC phase voltage amplitude	2.69 kV
AC current amplitude	309 A
Cells per arm	6
Switching freq.	2 kHz
DC Inductance:	2.5 mH
AC Inductance:	0.75 mH
Grid Inductance:	1.4 mH (0.05 p.u.)
DC load resistance	28.8 $\Omega$

A 40 ms operation sequence is implemented in both models for comparison. At 10 ms,  $i_{dc.ref}$  steps from 0 A to 200 A. At 20 ms, dc P-N short circuit is applied and then cleared at 25 ms. At 30 ms,  $i_{dc.ref}$  steps from 0 A to 309 A. The total clock time for the SWM is about 80.1 s to execute 0.04s simulation time while AVM executes the run in only 0.9 s clock time. From the simulation results in Fig. 4, SWM and SVM show consistent waveforms which validate the AVM built described in this report. The AVM is able to represent similar behavior to that of the SWM while reducing the complexity and significantly improving simulation time associated with the SWM.

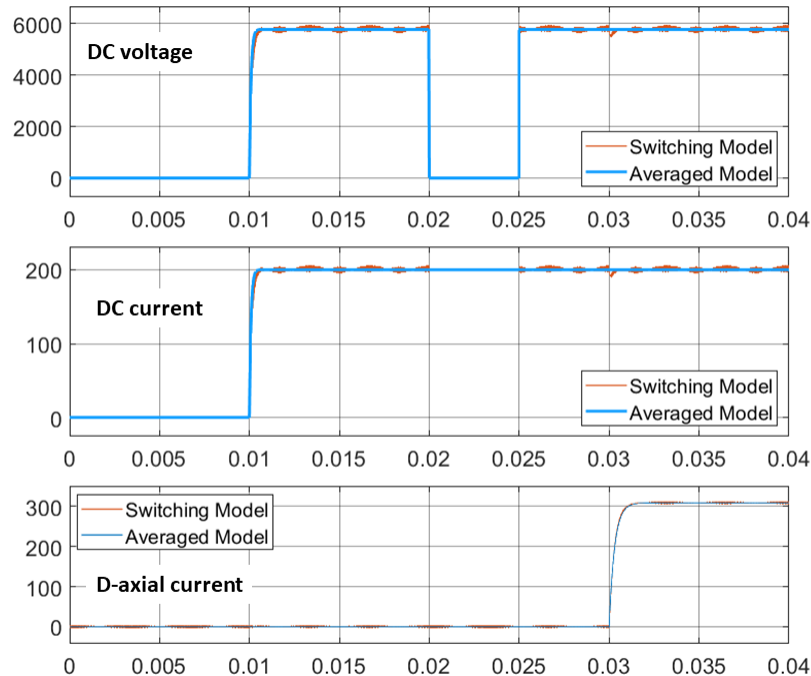


Fig. 4: MMC SWM and AVM simulation results comparison.

### 3 AVERAGE MODELING BY IMPEDANCE SHAPING

#### 3.1 MMC back to back tests

The AVM in this report is also tested in a back-to-back configuration, similar to past experimental tests conducted with the MMCs at CAPS. As shown in Fig. 5, two MMCs are in a back-to-back parallel connection. MMC1 is in a voltage control mode operation and establishes the voltage to the system acting as the source. MMC2 is in current control mode operation and acts as a constant current load. Connected at each MMC's dc-link, there is a RC filter where  $5 \Omega$  and series connected  $20 \mu\text{F}$  capacitor.

The AVM design is based on two sets of measured results. One data set is from Gunnar Chauncey's thesis in 2018 [1], which provides MMC1 and MMC2's impedance, measured from both CHIL testing and hardware testing. Another data set is from CHIL test results, which provides time domain voltage step and current step transients. Both the data sets are used in the same model with the same control. The objectives of the AVM is to match its impedance and then verify the time domain transient.

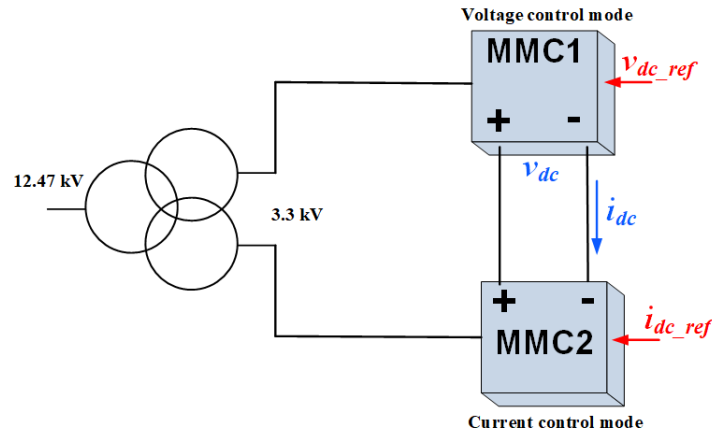


Fig. 5: MMC back to back testbed configuration.

### 3.2 Impedance shaping for current control mode MMC

The AVM in current control mode is shown in Fig. 6.  $K_{PWM}$  is the MMC plant gain, which is  $0.5NV_{cell}$  for the dc modulation.  $R_d$  is the reactive damping coefficient. The current controller  $G_{ci} = K_{pi} + \frac{K_{ii}}{s}$ . In the current control mode, the dc-link voltage is considered constant since the voltage loop is typically slower than the inner current loop and ideally  $Z_{MMC1}$  is large enough.

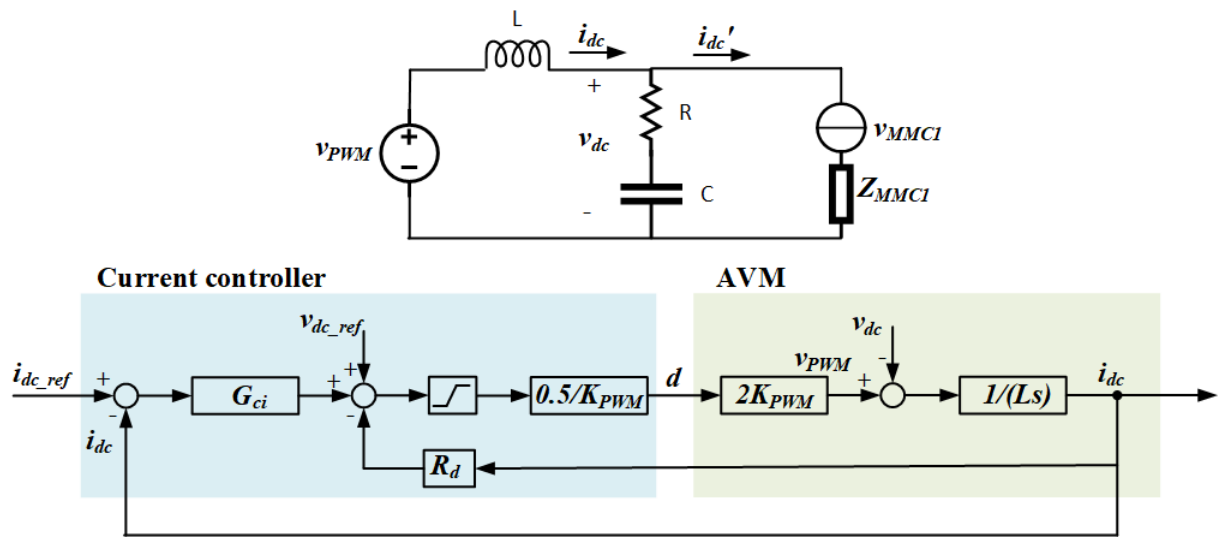


Fig. 6: AVM at current control mode.

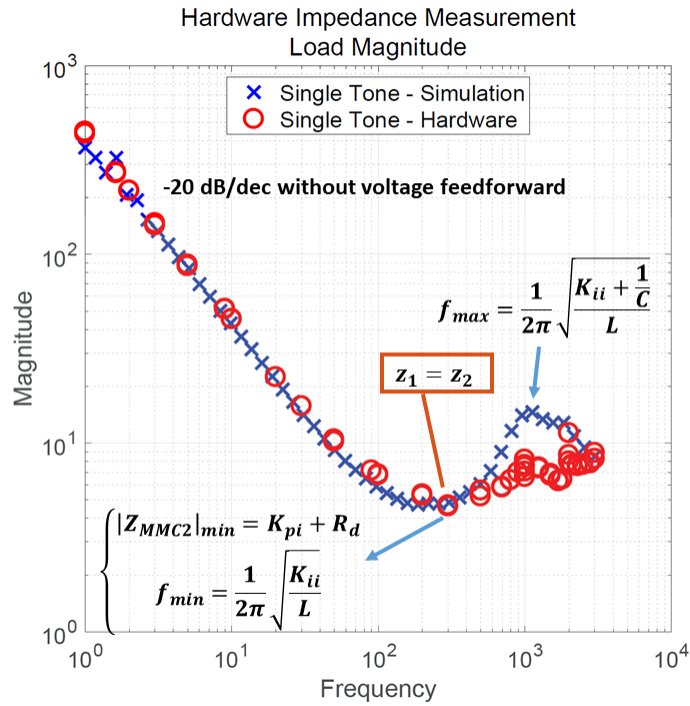


Fig. 7: Current control mode MMC impedance from test [1].

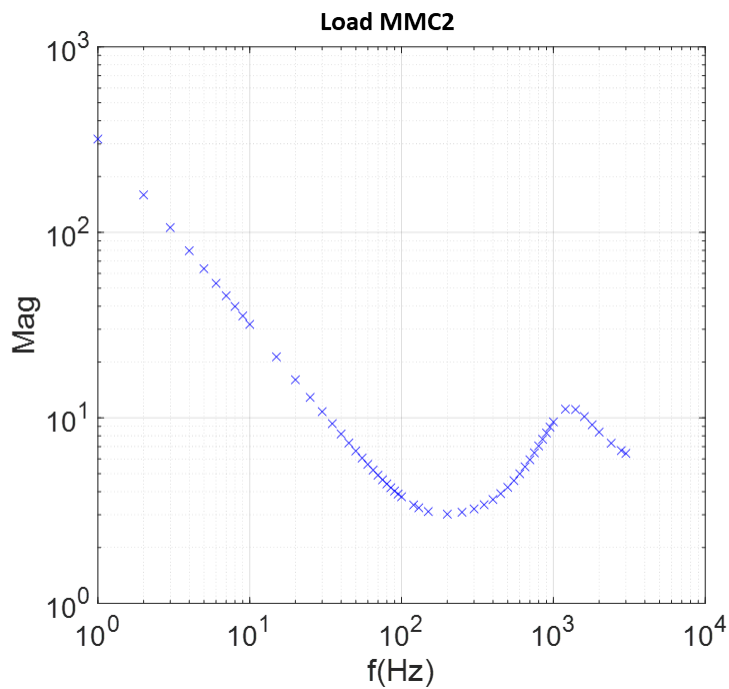


Fig. 8: Current control mode MMC impedance measurement from AVM.

Fig. 7 provides the current control mode MMC impedance calculation from previous test. Three key information can be observed from the impedance measurement. Impedance shaping can be implemented by changing parameters  $K_{pi} + R_d$  and  $K_{ii}$ .

(1) The magnitude reduces by -20 dB/dec with the frequency at low frequencies, which means there is no voltage feed forward control in the current loop. The reference voltage is added to the current controller output instead, as shown in Fig. 6. If there is a voltage feed forward control, the attenuation will be -40 dB/dec.

(2) The impedance lower than 1 kHz is given by (3), which is similar to a RLC in series circuit.

$$Z = \frac{v_{dc}}{i_{dc}} = sL + K_{pi} + R_d + \frac{K_{ii}}{s} \quad (3)$$

The impedance zeros are derived in (4), and the magnitude is in (5). When the control parameters  $K_p + R_d$  and  $K_i$  changes, the zeros changes from real numbers to imaginary numbers, and the impedance shape changes in the frequency domain, as shown in Fig. 9. When  $\omega^2 L = K_{ii}$ , the impedance magnitude is at its minimum value  $K_{pi} + R_d$ . Observed from the current control mode MMC impedance from test Fig. 7, the two zeros are the same.

$$z_{1,2} = \frac{-K_{pi} - R_d \pm \sqrt{(K_{pi} + R_d)^2 - 4LK_{ii}}}{2L} \quad (4)$$

$$|Z_{MMC2}(\omega)| = \sqrt{(K_{pi} + R_d)^2 + (\omega L - \frac{K_{ii}}{\omega})^2} \quad (5)$$

(3) The RC filter impact starts from 1 kHz, and the MMC2 impedance is provided by (6). The frequency for the maximum magnitude can be derived from the impedance poles, which is  $\sqrt{\frac{K_{ii} + \frac{1}{C}}{L}}$ .

$$Z_{MMC2} = \frac{v_{dc}}{i'_{dc}} = (sL + K_{pi} + R_d + \frac{K_{ii}}{s}) || (R + \frac{1}{Cs}) \quad (6)$$

After the impedance shaping, the current controller parameters are designed,  $K_{pi} = 4$ ,  $R_d = 1$ , and  $K_{ii} = 2960$ . For the MMC2 impedance measurement in the AVM, the B2B testbed was run at 5 kV, 200 A, and a 5% voltage disturbance is added in series with  $v_{MMC1}$ . The measured current control mode impedance for MMC2 is in Fig. 8. The impedance measurement from the AVM is consistent with the test results.

### 3.3 Impedance shaping for voltage control mode MMC

The AVM in voltage control mode is shown in Fig. 10. The current feed forward through a low pass filter is added in the voltage loop. The voltage controller  $G_{cv} = K_{pv} + \frac{K_{iv}}{s}$ . Since the RC filter impedance is much larger than the load MMC impedance  $Z_{MMC2}$ , it is neglected in the voltage control mode AVM impedance shaping.  $i_{dc}$  is considered the same as  $i'_{dc}$ .

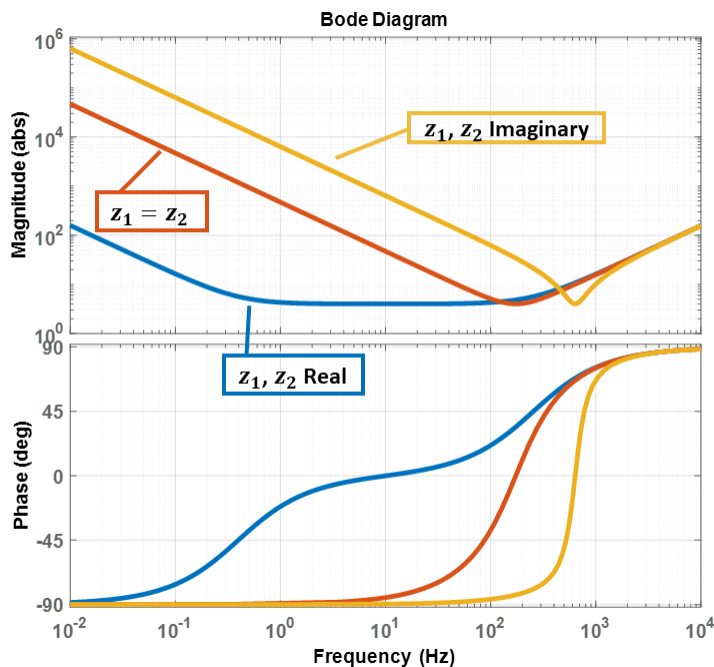


Fig. 9: Current control mode MMC impedance shaping with different zeros.

The impedance of the voltage control mode MMC is shown in (7), where  $G_i = \frac{G_{ci}}{G_{ci} + Ls + R_d}$  is the closed current loop transfer function.

$$Z_{MMC1} = \frac{Z_{MMC2}}{1 + G_{cv}G_iZ_{MMC2}} \quad (7)$$

Observed from the current control mode MMC impedance from test Fig. 11, there are four sections. Section (1) is -40 dB/sec at low frequency, which means that there is current feed forward enabled. The attenuation would be -20 dB/sec if there is no current feed forward control. Section (2) is the voltage controller performance, section (3) is the inner current loop controller, and section (4) is the dc inductor impact. The voltage control mode MMC impedance shaping is implemented based on each section's design.

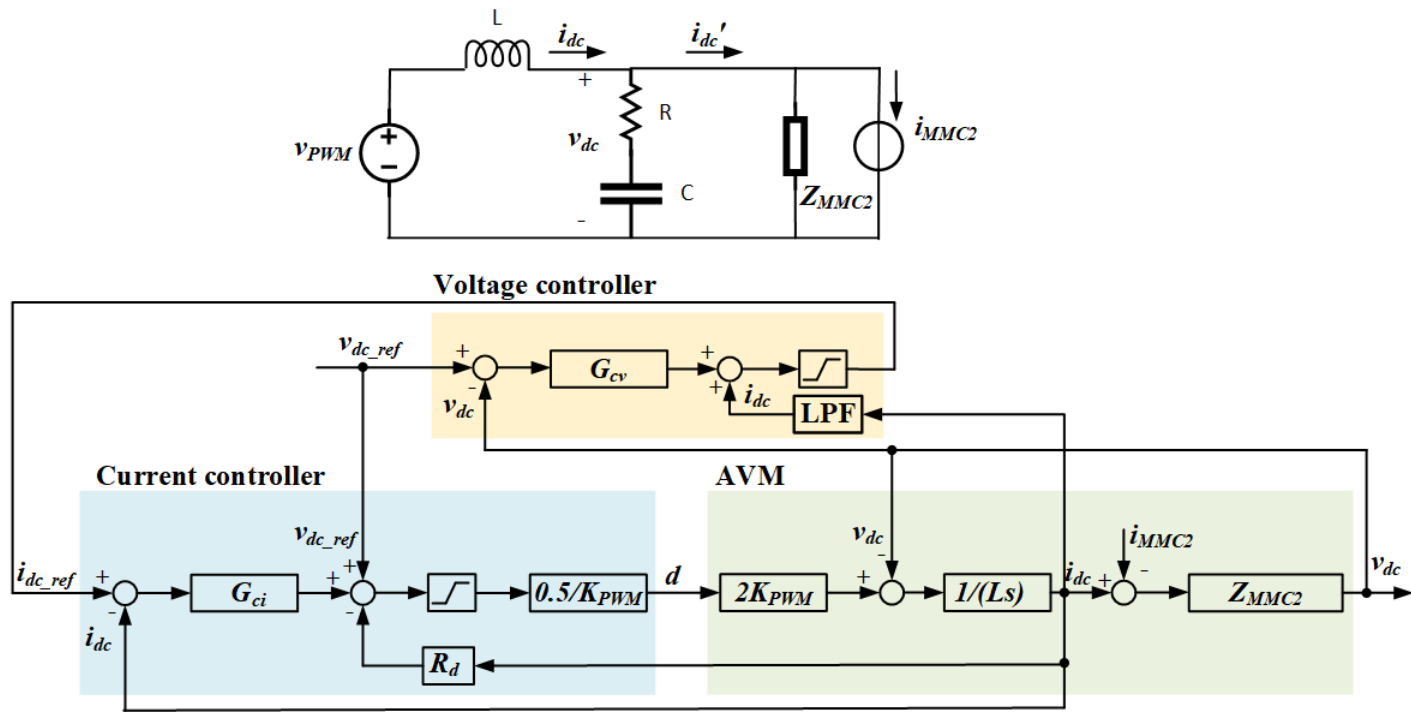


Fig. 10: AVM at voltage control mode.

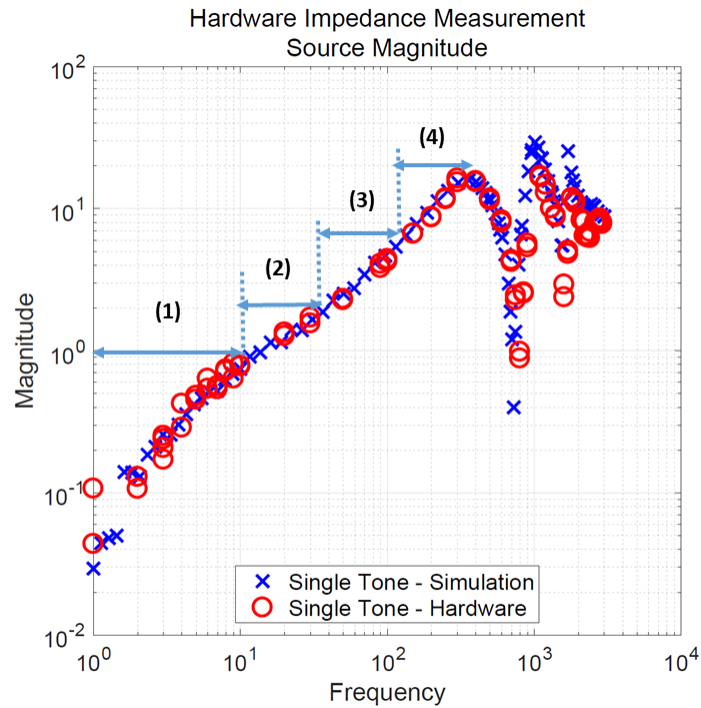


Fig. 11: Voltage control mode MMC impedance from test [1].

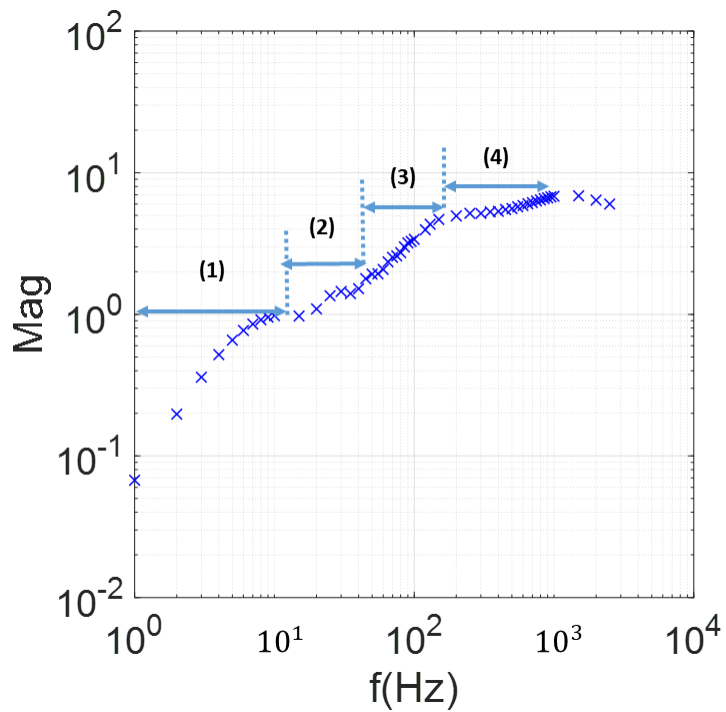


Fig. 12: Voltage control mode MMC impedance measurement from AVM.

For the MMC1 impedance measurement in the AVM, the B2B test is executed at 5 kV, 200 A, and a 5% current disturbance is added in parallel with  $i_{MMC2}$ . The measured voltage control mode impedance for MMC1 is in Fig. 12. The impedance measurement from the AVM is consistent with the test results up to 300 Hz. The higher frequency impedance shaping still needs further investigation and improvement.

## 4 AVERAGE MODEL VERIFICATION AND VALIDATION

The Matlab/Simulink models are included with this report, and the model description document is given by [3].

### 4.1 MMC current transient

The simulation result of the average model is compared against the measured result using control hardware-in-the loop (CHIL) test. A comparison of the current step response example is shown in Fig. 13, where the current changes from 0 to 200 A and the dc voltage is controlled to 5 kV by MMC1. The peak time, overshoot, and settling time are measured and compared.

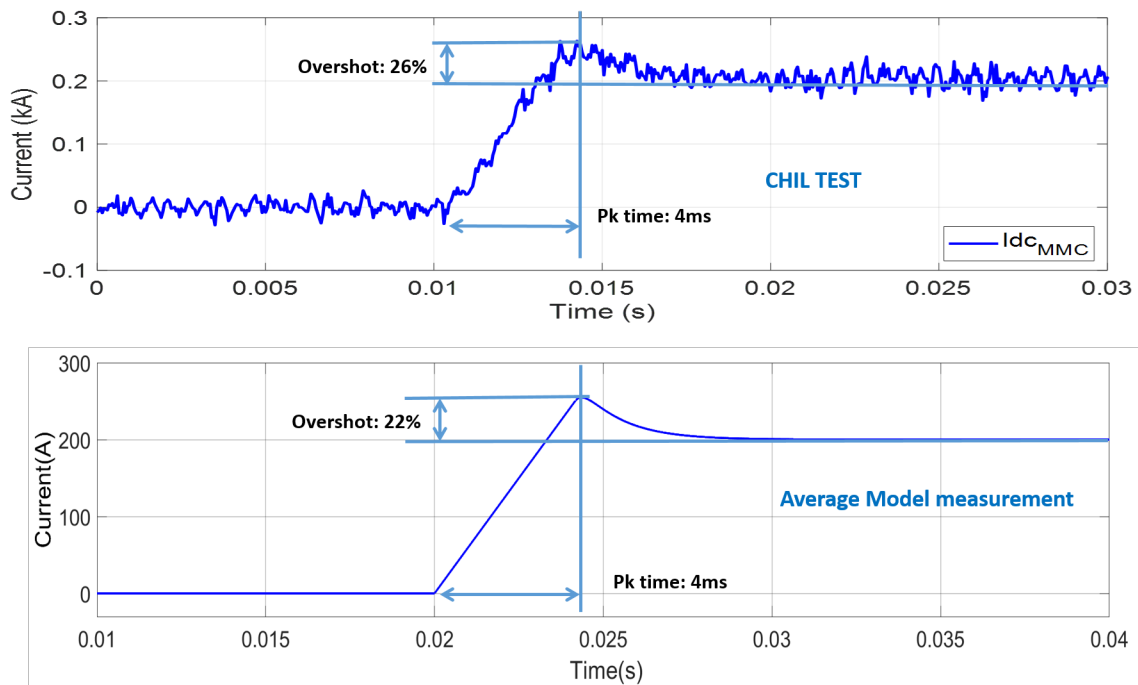


Fig. 13: Current control mode MMC current 0-200 A step response comparison (at 5 kV).

Batch CHIL experiments were performed to verify the AVM in the operation space. In the CHIL experiments, DC current step response was measured with current reference range from 5 A to 200A, in 10 A interval. At each reference, the experiment was repeated 100 times. 11-points

digital medium filter was applied to the recorded current waveform to eliminate the influence of high frequency distortion on rise time measurement. The measured rise time from AVM and the CHIL are shown in Fig. 14. The data points marked by the blue cross are CHIL results and the data with green diamond marker are from AVM. The error of rise time between AVM results and the mean value of 100 CHIL results at each current step is shown in Fig. 15. The average of the absolute value of the error is 12%.

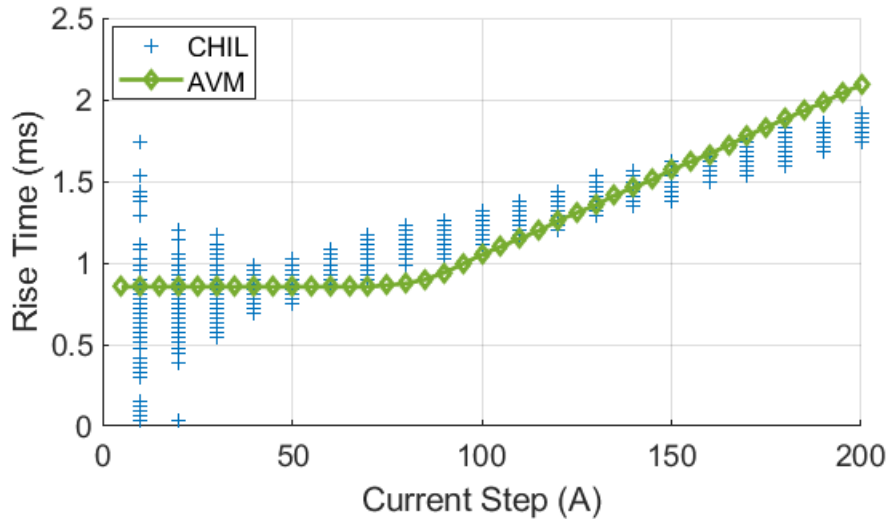


Fig. 14: Current transient comparison between AVM and CHIL.

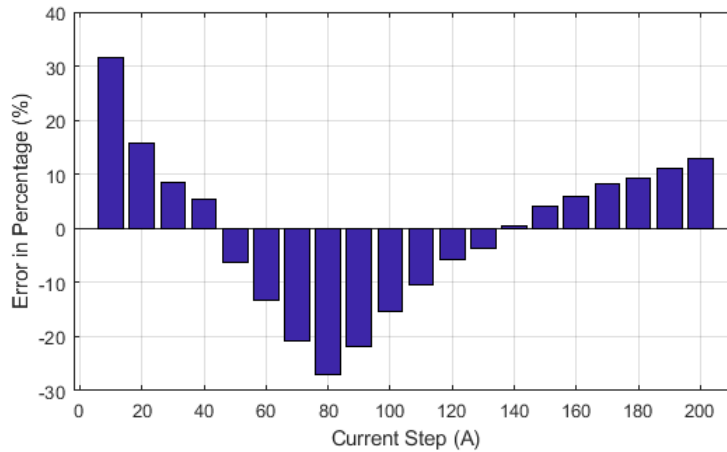


Fig. 15: Percentage of error in rise time between CHIL and AVM.

## 4.2 MMC voltage transient

The voltage step response example is shown in Fig. 16, where the voltage changes from 0 to 5 kV and the dc current is 200 A controlled by MMC2. The voltage transient is a typical slope response without any overshoot. So the rising time is selected to represent the characteristics and implement the V&V.

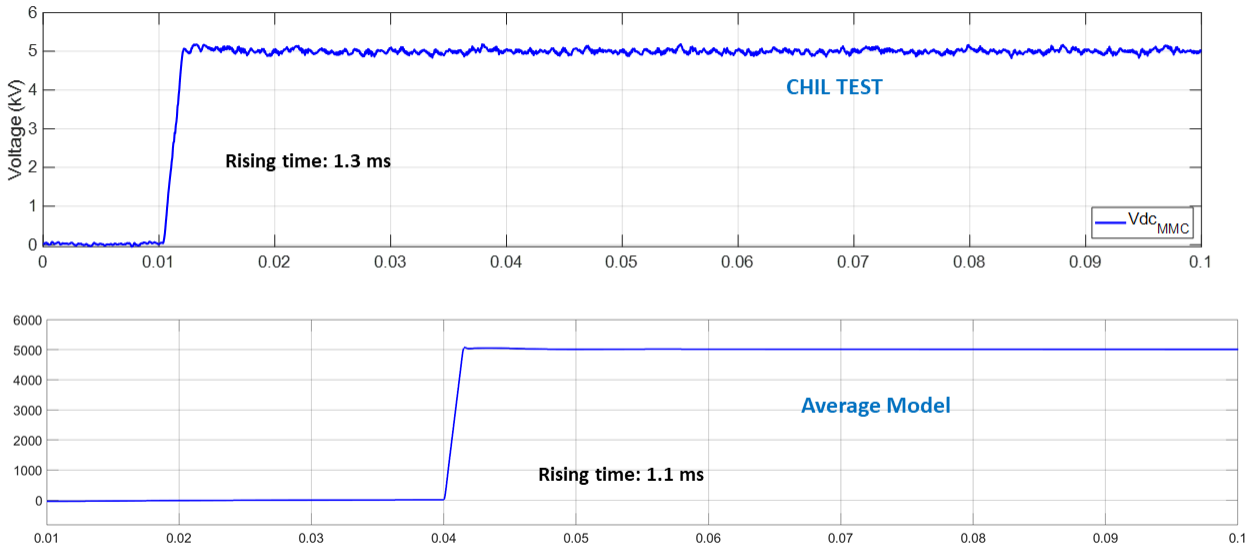


Fig. 16: Voltage control mode MMC voltage 0-5 kV step response comparison (at 200 A).

Different cases are designed to verify the voltage transient with different initial voltage and step voltage, which are listed in Table 2. All 21 cases are implemented in both the AVM and the CHIL at 50-200 dc current levels.

The voltage transient characteristics comparison between AVM and CHIL are shown in Fig. 17. The testing cases in Table 2 were executed. The blue dotted line is the AVM simulation results, which is the same at different dc currents. CHIL test results also have very similar results between different dc currents. The rising time matches well between the AVM and CHIL, where the maximum error is below 20%, as shown in Fig. 17.

The voltage transient is a slope response, the rising time is characterized for the comparison.

- Rising time is independent from the dc current;
- Rising time changes linearly with the voltage step value. In average, the coefficient is  $0.23 \mu\text{s}/V$  in AVM and  $0.27 \mu\text{s}/V$  in CHIL;
- The AVM error is about 15% compared to CHIL results.

Table 2: Voltage transient cases

<b>Cases No.</b>	<b>Initial voltage (V)</b>	<b>Target Voltage (V)</b>	<b>Voltage step (V)</b>
1	0	1000	1000
2	0	2000	2000
3	1000	2000	1000
4	0	3000	3000
5	1000	3000	2000
6	2000	3000	1000
7	0	4000	4000
8	1000	4000	3000
9	2000	4000	2000
10	3000	4000	1000
1	0	5000	5000
2	1000	5000	4000
3	2000	5000	3000
4	3000	5000	2000
5	4000	5000	1000
6	0	6000	6000
7	1000	6000	5000
8	2000	6000	4000
9	3000	6000	3000
10	4000	6000	2000
10	5000	6000	1000

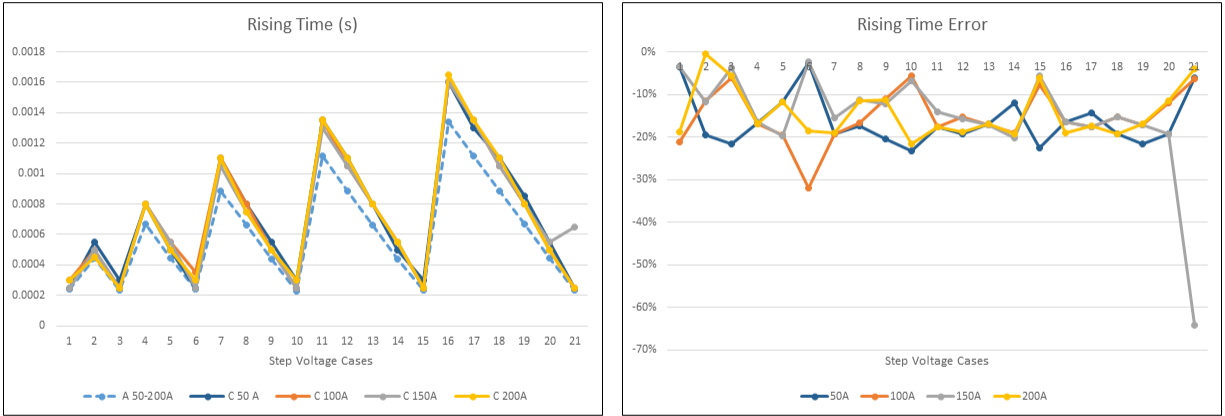


Fig. 17: Voltage transient comparison between AVM and CHIL.

### 4.3 MMC short circuit operation

The short circuit test configuration is shown in Fig. 18. MMC is running in voltage control mode and open circuit. Results from the short circuit result at 5 kV is shown in Fig. 19.

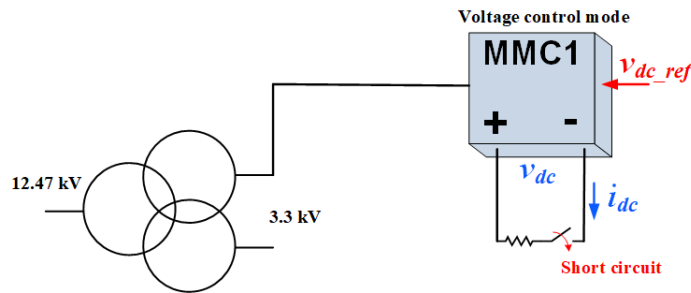


Fig. 18: MMC short circuit test configuration.

For the validation, both AVM and CHIL are implemented for 1-5.5 kV short circuit operation. The fault current peak, rising time, and falling time are characterized for the comparison, as shown in Fig. 20. The errors for the fault current comparison are shown in Fig. 21. The blue dash line is the overall error, which is the square root of the three aspects' square sum.

For the AVM short circuit transient, the overall fault current error is the square root of the square sum average of peak, rising time, and falling time errors.

- The fault current peak increases nearly linearly with the DC bus voltage. The error between the AVM and CHIL is less than 4%.
- Rising time and falling time are relatively constant with different DC bus voltages. The error between the AVM and CHIL is between 5%-40%.

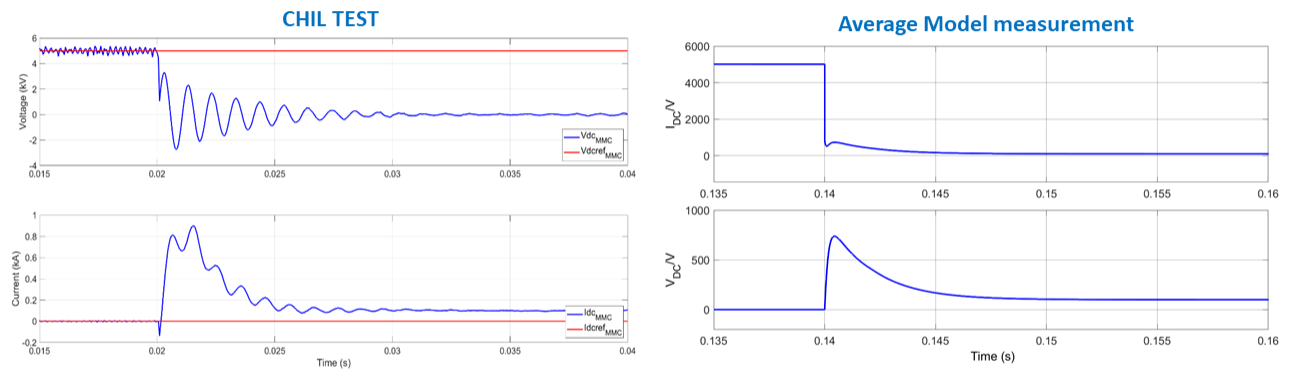


Fig. 19: Single MMC voltage control mode short circuit comparison (at 5 kV open circuit).

- AVM provides good results for 2-5 kV dc bus short circuit transient, where the overall error is around 20%.

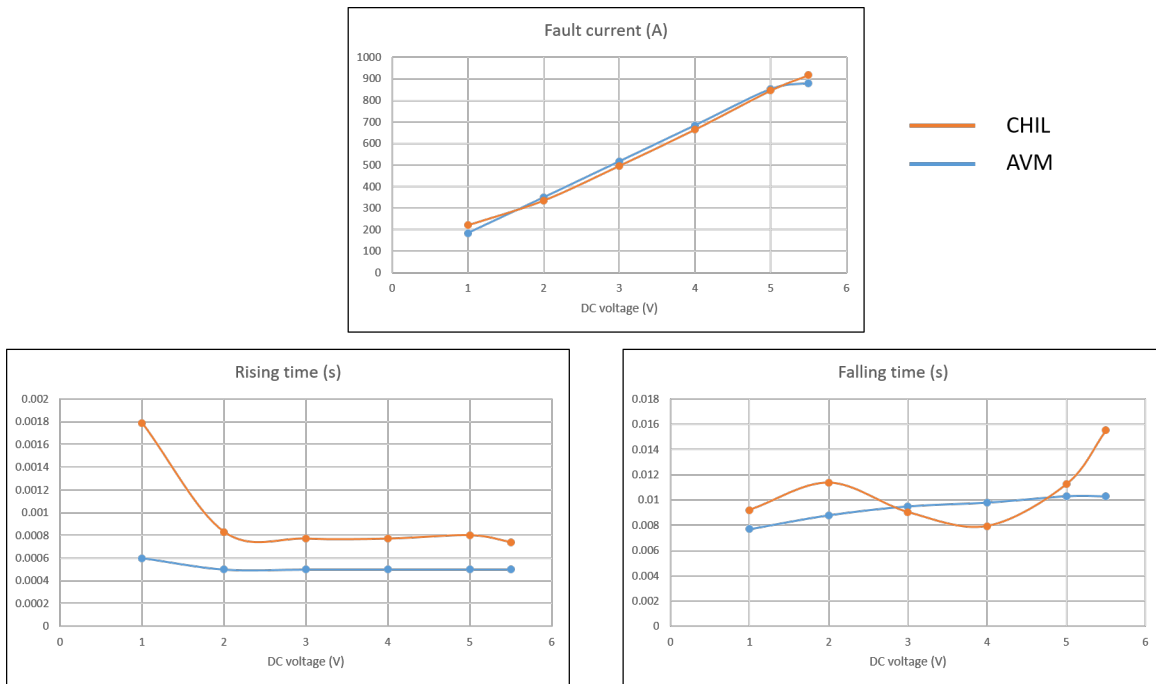


Fig. 20: Short circuit comparison between AVM and CHIL.

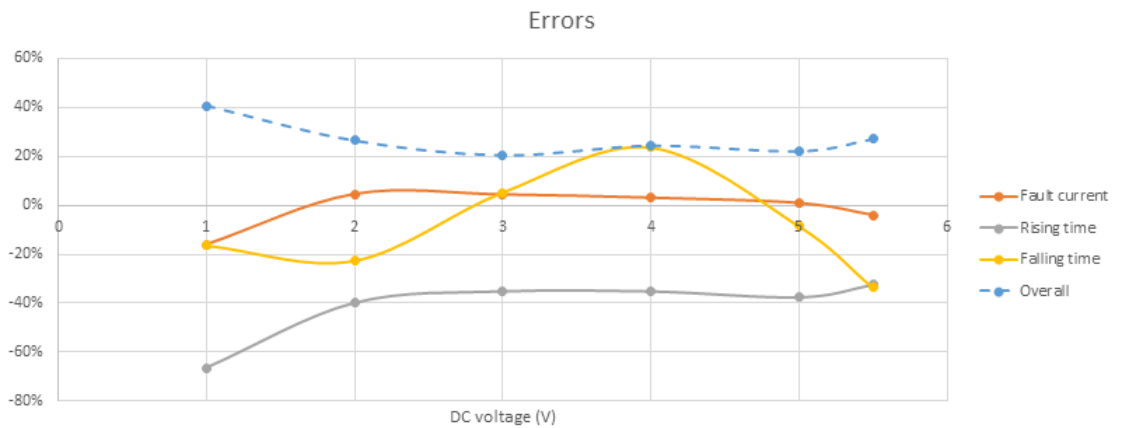


Fig. 21: AVM short circuit operation errors.

## 5 CONCLUSION

- For the current controlled MMC, AVM developed in this report is able to shape the impedance up to 3 kHz.
- For the voltage controlled MMC, AVM developed in this report is able to shape the impedance up to 300 Hz.
- For the current transient, the step response is decided by the current step magnitude and independent from the initial current value and DC bus voltage. In the range of 10-200A, the averaged absolute error in rise time is 12%.
- For the voltage transient, the slope response is independent from the initial voltage and the DC current, and the rising time increases linearly with the step voltage magnitude. The AVM is validated with about 15% error for 0-6 kV voltage step transient.
- For the DC bus short circuit operation, the fault current peak increases linearly with the DC bus voltage. The overall fault current error is the square root of the square sum average of peak, rising time, and falling time errors. AVM is validated for 2-5 kV dc bus short circuit transient, where the peak current error is within 4% and the overall error is around 20%.

## 6 FUTURE WORK

During the model validation process, we discovered that when repeating a test at the exactly same condition for multiple times the test results can show a distribution. Fig. 22 presents the statistical CHIL results of the rise time from 2000 tests with 5A step and 50A step in back to back configuration. The result with 50A step can fit into a normal distribution with relative standard deviation of 6.6%. This result means 68%, or one  $\sigma$ , of data is within the 6.6% range of the mean value, and 99.7%, or  $3\sigma$ , of data is within 20% range of the mean value. However, the test results from 5A step presents a much larger deviation, which suggests that the rise time of this converter may not be "modelable" at 5A. Similar phenomenon can also be found in experiment results with a commercial MMC, as shown in Fig. 23.

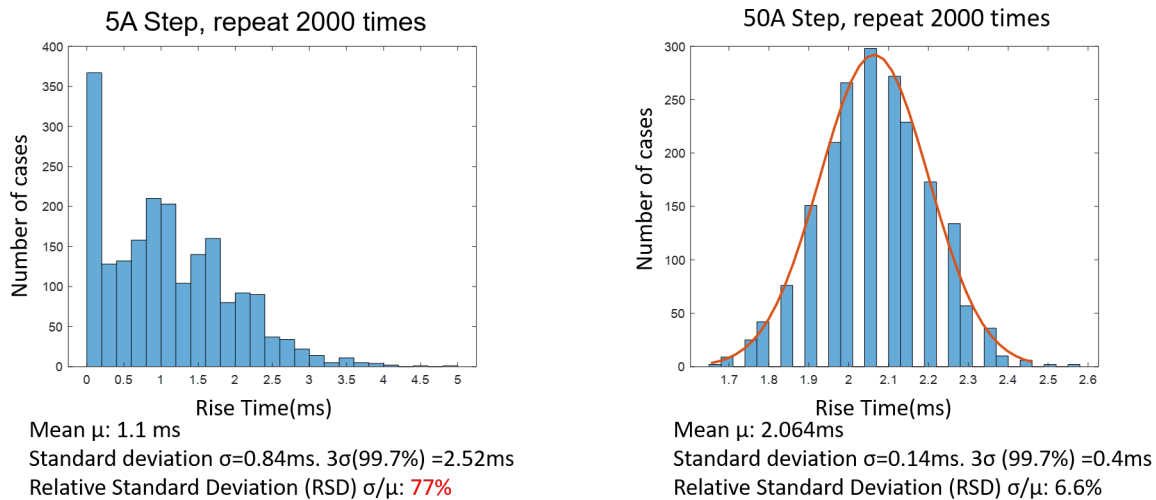


Fig. 22: Statistic of measured rise time in CHIL.

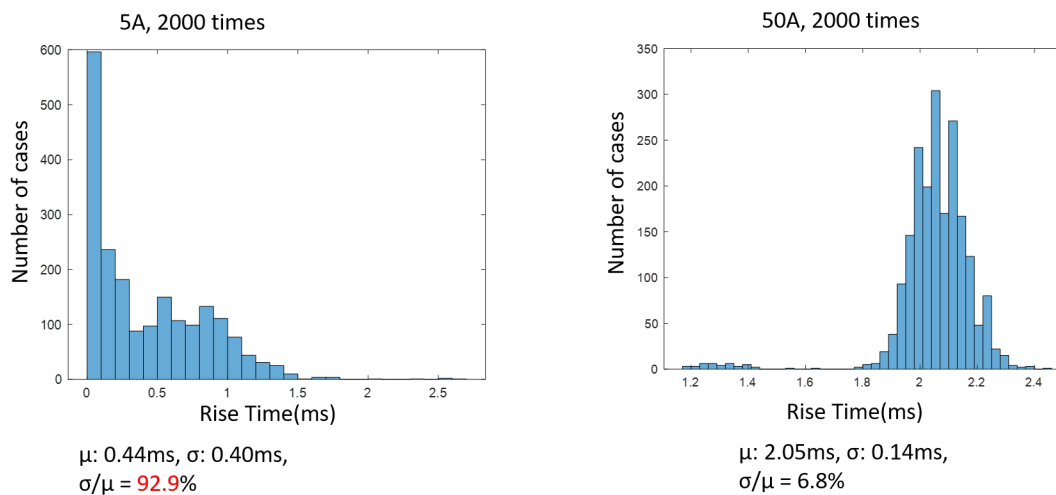


Fig. 23: Statistic of measured rise time from experiments with two B2B 1.25MW MMCs.

Therefore, there is a need to further investigate this phenomenon by:

- Developing standard test procedure to identify the subset of the operation space that can or can not be modeled. Fig.24 presents an example of possible result from such study.
- Searching for suitable mathematical tools to quantify the degree of modelability.
- Developing design and control methods to increase the modelability of power converters.

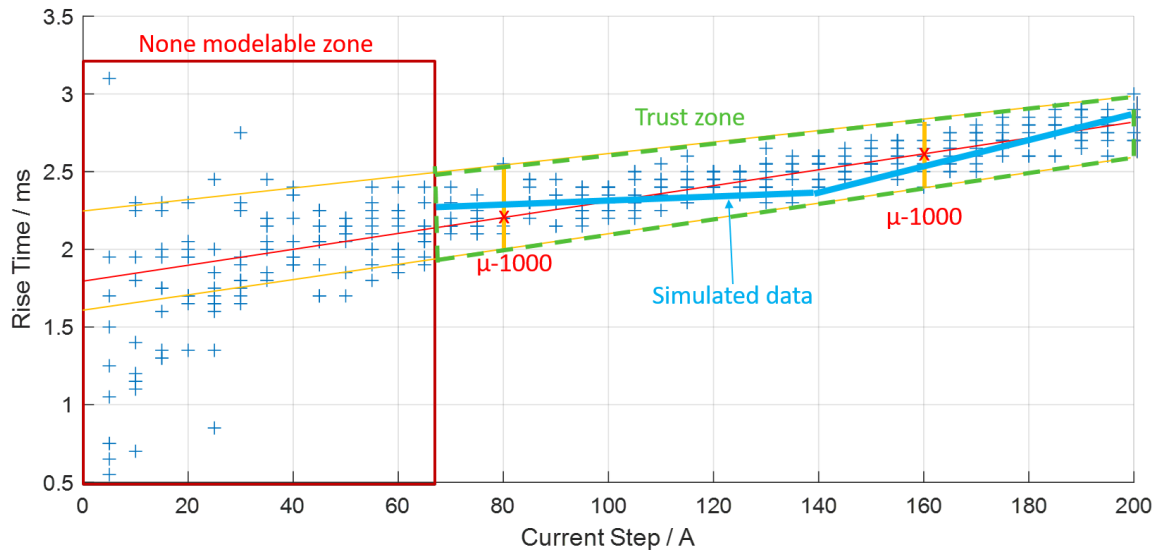


Fig. 24: Example of a power converter modelability study

## REFERENCES

- [1] Gunnar Chauncey. Impedance measurement techniques in noisy medium voltage power hardware-in-the-loop environments. Master's thesis, Florida State University, 2018.
- [2] M. M. Steurer, K. Schoder, O. Faruque, D. Soto, M. Bosworth, M. Sloderbeck, F. Bogdan, J. Hauer, M. Winkelkemper, L. Schwager, and P. Blaszczyk. Multifunctional Megawatt-Scale Medium Voltage DC Test Bed Based on Modular Multilevel Converter Technology. *IEEE Transactions on Transportation Electrification*, 2(4):597–606, Dec 2016.
- [3] L. Wang, Y. Shi, D. Soto, J. Langston, K. Schoder, and M. Steurer. Modular multi-level converter average value model. Technical report, The Electric Ship Research and Development Consortium, November 2019.

## A ATTACHED MATLAB MODEL LIST

- AVM for current control mode MMC: *Run\_I.m, MMC\_AVM\_I.slx*;
- AVM for voltage control mode MMC: *Run\_V.m, MMC\_AVM\_V.slx*;
- AVM for voltage control mode MMC short circuit: *Run\_V\_SC.m, MMC\_AVM\_sc.slx*.